Measuring Storm Surge with an Airborne Wide-Swath Radar Altimeter

C. W. WRIGHT,* E. J. WALSH,* W. B. KRABILL,* W. A. SHAFFER,+ S. R. BAIG,# M. PENG,@ L. J. PIETRAFESA,@ A. W. GARCIA,& F. D. MARKS JR.,** P. G. BLACK,**,@@ J. SONNTAG,++ AND B. D. BECKLEY##

* *NASA Goddard Space Flight Center, Wallops Island, Virginia*
+ *NOAA/National Weather Service, Silver Spring, Maryland*
# *NOAA/Tropical Prediction Center, Miami, Florida*
@ *College of Physical and Mathematical Sciences, North Carolina State University at Raleigh, Raleigh, North Carolina*
& *Coastal and Hydraulic Laboratory, U.S. Army Engineer R&D Center, Vicksburg, Mississippi*
** *NOAA/AOML/Hurricane Research Division, Miami, Florida*
++ *EG&G Technical Services, Inc., Wallops Island, Virginia*
SGT Incorporated, Greenbelt, Maryland

(Manuscript received 8 February 2008, in final form 6 January 2009)

ABSTRACT

Over the years, hurricane track forecasts and storm surge models, as well the digital terrain and bathymetry data they depend on, have improved significantly. Strides have also been made in the knowledge of the detailed variation of the surface wind field driving the surge. The area of least improvement has been in obtaining data on the temporal/spatial evolution of the mound of water that the hurricane wind and waves push against the shore to evaluate the performance of the numerical models. Tide gauges in the vicinity of the landfall are frequently destroyed by the surge. Survey crews dispatched after the event provide no temporal information and only indirect indications of the maximum water level over land. The landfall of Hurricane Bonnie on 26 August 1998, with a surge less than 2 m, provided an excellent opportunity to demonstrate the potential benefits of direct airborne measurement of the temporal/spatial evolution of the water level over a large area. Despite a 160-m variation in aircraft altitude, an 11.5-m variation in the elevation of the mean sea surface relative to the ellipsoid over the flight track, and the tidal variation over the 5-h data acquisition interval, a survey-quality global positioning system (GPS) aircraft trajectory allowed the NASA scanning radar altimeter carried by a NOAA hurricane research aircraft to demonstrate that an airborne wide-swath radar altimeter could produce targeted measurements of storm surge that would provide an absolute standard for assessing the accuracy of numerical storm surge models.

1. Introduction

The National Aeronautics and Space Administration (NASA) scanning radar altimeter (SRA) has a long heritage in measuring the energetic portion of the sea surface directional wave spectrum (Walsh et al. 1985, 1989, 1996, 2002; Wright et al. 2001, Black et al. 2007). SRA wave spectra have been used to assess the performance of the WaveWatch III numerical wave model (Moon et al. 2003; Fan et al. 2009). This paper demonstrates that an airborne wide-swath radar altimeter could also routinely provide targeted measurements of storm surge for assessing and improving the performance of numerical storm surge models.

As a hurricane makes landfall, its wind and waves push a mound of water against the shore on the right side of the eye. Offshore wind can depress the water level to the left of the eye. In this paper, we will use the term storm surge to refer to the deviation of the water level from its predicted value in the absence of the hurricane.

Some of the factors affecting the height and extent of the storm surge are the maximum wind speed, the radius of maximum wind, the forward speed of the storm, its angle of track relative to the coastline, and

@@ Current affiliation: Science Applications International Corporation, Monterey, California.

Corresponding author address: Edward J. Walsh, R/PSD3, NOAA/Earth System Research Laboratory, 325 Broadway, Boulder, CO 80305-3328.
E-mail: edward.walsh@noaa.gov

DOI: 10.1175/2009JTECHO627.1

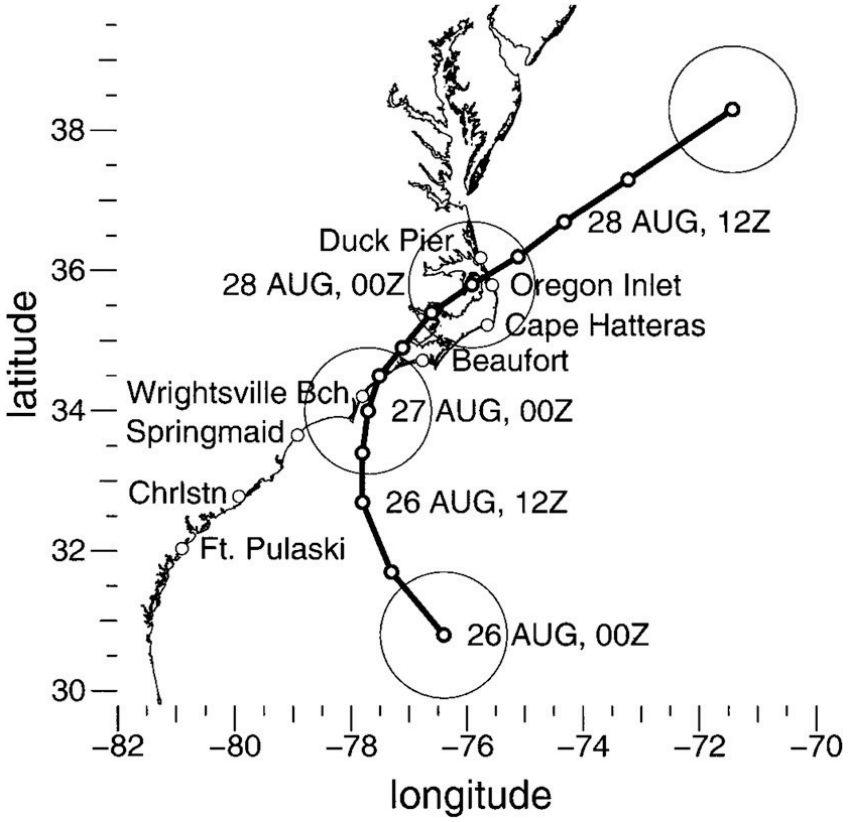

FIG. 1. NHC best-track eye locations for Hurricane Bonnie (thick circles) in 1998. Thin circles indicate tide gauge locations at Duck Pier (36.18°N, 75.75°W), Oregon Inlet (35.79°N, 75.55°W), Cape Hatteras (35.22°N, 75.63°W), Beaufort (34.72°N, 76.76°W), in North Carolina; Springmaid Pier (33.65°N, 78.92°W) and Charleston (32.78°N, 79.92°W) in South Carolina; and Fort Pulaski (32.03°N, 80.90°W) in Georgia. The tide gauge at Wrightsville Beach (34.21°N, 77.79°W) was not placed in operation until 2004.

the characteristics of the bathymetry and coastline. Over the years, forecasts of hurricane position and timing, as well as the surge models and the digital terrain and bathymetry data they depend on, have improved significantly. Strides have also been made in the knowledge of the surface wind field from airborne measurements using GPS dropwindsondes and stepped frequency microwave radiometers (Powell et al. 1998, 2003; Uhlhorn and Black 2003; Uhlhorn et al. 2007) as well as wind data gathered from temporary towers set up along the coast in the hurricane's projected path (Schroeder and Smith 2003).

The area of least improvement has been in obtaining detailed data on the temporal/spatial evolution of the water level to evaluate the performance of the numerical models. Tide gauges in the vicinity of the landfall are useful in determining this variation, but they are frequently destroyed by the surge. Survey crews dispatched after the event provide no temporal information and only indirect indications of the maximum surge envelope over land (Fritz et al. 2007; FEMA 2006).

The landfall of Hurricane Bonnie on 26 August 1998 provided an excellent opportunity to demonstrate the potential benefits of direct airborne measurement of the temporal/spatial evolution of storm surge. Bonnie was a slow moving storm with a large radius of maximum wind, minimizing both the temporal and spatial gradients. The peak of the Hurricane Bonnie storm surge was less than 2 m, providing an opportunity to demonstrate that even a minimal surge can be well documented.

Figures 1 and 2 provide an overview to put the measurements in perspective. Figure 1 indicates the National Hurricane Center (NHC) best-track eye locations for Hurricane Bonnie at 6-h intervals from 0000 UTC 26 August to 0000 UTC 29 August 1998 (available online at http://www.nhc.noaa.gov/1998bonnie.html). Circles of 100-km radius have been placed around the four 0000 UTC eye locations because that was the approximate radius of maximum wind on 26 August when the SRA observations were made. The numerical models indicate that the surge peaked on the east side of Cape Fear, North Carolina, in the afternoon of 26 August and

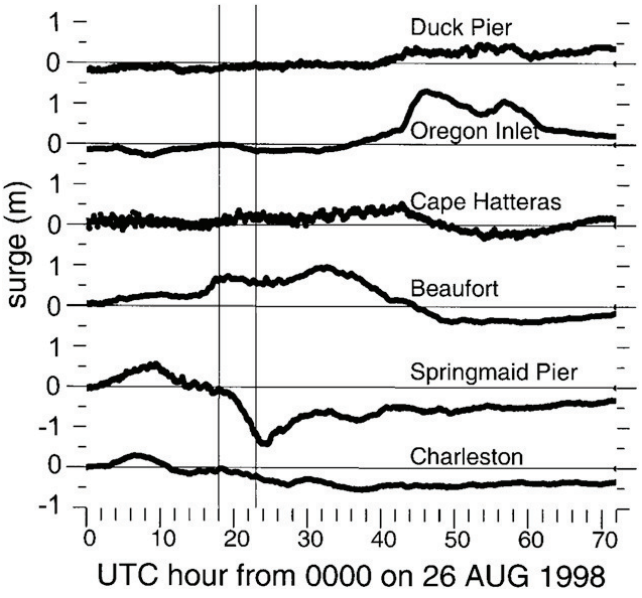

FIG. 2. Tide gauge surge records with the interval of the SRA observations (1800–2300 UTC) indicated by the vertical lines.

then slowly diminished as it shifted north along the North Carolina coast.

The small, thin circles indicate tide gauge locations. The Wrightsville Beach, North Carolina, tide gauge was not in operation during the Bonnie landfall, but we will extrapolate a tide prediction for that location. Figure 2 shows the surge record from six of the tide gauges. The most dramatic water level variation seen by the gauges during the SRA measurement interval was the depression of the water surface caused by the offshore wind at Springmaid Pier, South Carolina. It is interesting that the largest positive surge observed by the gauges occurred at the Oregon Inlet sheltered location. When the wind was onshore, water slowly entered Pamlico Sound through gaps in the Outer Banks and was pushed to the west. When the onshore wind diminished and began to reverse late on 27 August, the water flowed back to the east but could not readily escape, and it piled up against the Outer Banks.

2. The mean sea surface

Figure 3 indicates the track of the National Oceanic and Atmospheric Administration (NOAA) Aircraft Operations Center (AOC) WP-3D hurricane research aircraft (N43RF) carrying the NASA SRA on 26 August 1998 superimposed on elevation contours of the NASA Goddard Space Flight Center mean sea surface model (GSFC00.1_MSS, hereafter MSS; Wang 2001) relative to the Ocean Topography Experiment (TOPEX)/Poseidon (T/P) standard reference ellipsoid (Tapley et al. 1994) used to approximate the overall shape of the earth.

The MSS has been blended with the geoid so that its contours extend over land. The geoid is the gravitational equipotential surface determined by the mass distribution of the earth. The sea surface would conform to the geoid if the earth was not rotating and there were no currents or external forces acting on it such as the wind or the gravitational pulls of the moon and sun. The MSS differs from the geoid in that it incorporates the mean elevation of any currents, such as the Gulf Stream, and any constant tides.

Figure 3 indicates that the sea surface mean elevation varies significantly off the mid-Atlantic coast of the United States with a range of 11.5 m over the aircraft track. The high point was 33.5 m below the T/P ellipsoid at position E and the low point was 45 m below the ellipsoid at position H. The continental shelf break is in the vicinity of the −41-m contour.

3. Sea surface topography measurements

Figure 4 shows the measurement geometry of the SRA during the landfall flight. The SRA scanned a 1° (two way) beam from left to right through the nadir point in the plane perpendicular to the aircraft heading and measured the slant range to 64 points over a swath width equal to 0.8 times the aircraft height. The mean altitude of about 2140 m resulted in a 1712-m swath and a 37-m footprint. The 5.5-Hz scan rate and 120 m s^{-1} nominal ground speed produced an along-track separation of 22 m between consecutive 64-point cross-track raster scan lines. The boresight angles of the 64 cross-track antenna beam positions were spaced at 0.7° intervals so that adjacent locations were separated by 26 m near the nadir point and 30 m near the edge of the swath.

The NOAA aircraft typically flies in a 2° nose-up pitch attitude and the SRA antenna was mounted looking aft by 2°, so it would generally scan through the nadir point during the flights. To obtain the vertical distances from the SRA antenna to the various positions across the swath, the SRA slant range measurements were multiplied by the cosine of the actual off-nadir pitch angle of the beams indicated by the aircraft inertial navigation system (INS) and by the cosine of the off-nadir beam boresight angles in the cross-track plane. Subtracting these vertical distances from the height of the antenna produced a topographic map of the surface.

The pitch attitude is generally quite stable unless the aircraft is initiating or terminating an altitude transition. But even in level flight, the roll attitude continually oscillates by several degrees. Any error in aircraft roll attitude added to the nominal cross-track boresight angles of the beams would make the sea surface appear to be

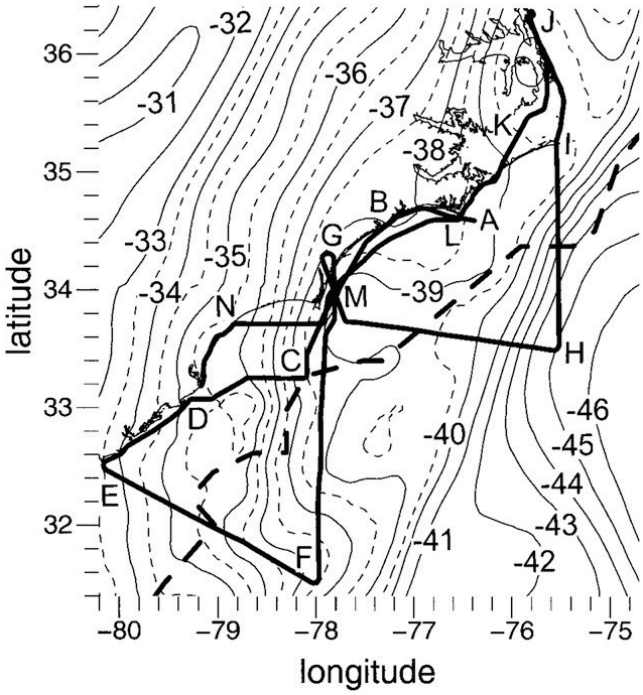

FIG. 3. NOAA aircraft track (thick line) on 26 Aug 1998, with the letters identifying a chronological sequence of positions. Thick dashed line is a piecewise linear approximation of the western edge of the Gulf Stream. The thin solid and dashed lines indicate the elevation (m) of the MSS relative to a reference ellipsoid.

tilted by the same amount. At a 2140-m height, a roll attitude error of only 0.2° would elevate one edge of the swath by 3 m and depress the other edge by the same amount. The INS is more accurate than that, but there is enough torsion in the airframe to cause the roll attitude of the SRA antenna mounted near the back of the aircraft to deviate from the roll attitude measured by the INS.

Figure 5 shows two grayscale-coded sea surface topographic maps produced from different processings of SRA data as the aircraft flew from east to west across Cape Lookout, North Carolina (34.58°N, 76.53°W; Fig. 3, point A). The SRA antenna scans in the plane perpendicular to the aircraft heading, but that is generally not perpendicular to the aircraft ground track. At Cape Lookout, the local wind was from the left side of the aircraft and the pilot pointed the nose of the aircraft about 14° to the left so that the cross-track component of airspeed would cancel the cross-track component of wind speed and the aircraft would maintain the desired course. This ''crab angle'' is apparent at the beginning and end of the sequence of scan lines shown in Fig. 5.

The significant wave height was about 4.6 m at Cape Lookout and the dominant wavelength was about 165 m. The grayscale spans just 5 m vertically to emphasize the surface tilts. The topography in the top map was generated using the aircraft roll attitude indicated by the INS. There were 16 occasions in the 17-km span of data shown in which torsion in the airframe induced erroneous sea surface tilts whose magnitude exceeded 0.2° (6-m elevation change across the swath). These are apparent in the top image by one edge of the swath becoming light while the other edge becomes dark. The largest roll excursion (−5°) occurred at 11.7 km, but it induced less airframe torsion than the more rapid 3.2° excursion at 15.6 km.

This problem can be greatly mitigated by assuming that a straight line fitted through the elevation points over the 1700-m swath should be horizontal and computing the antenna roll attitude rather than applying the INS roll. The bottom sea surface map in Fig. 5 was produced in that fashion and does not exhibit the sea surface tilts.

The bottom image in Fig. 5 is similar to Walsh et al. (2002, their Fig. 4) except that there are less data retained near the edge of the swath and most of the Cape Lookout terrain (between 6.5 and 9 km) is missing. This is because a higher signal level threshold was used for the storm surge measurements to reduce noise in the range measurements. Land has a significantly lower radar backscatter coefficient than water. The SRA antenna gain varied little over most of the swath but then rolled off rapidly, being 12 dB lower (two way) at the swath edges.

Because the highest-quality range measurements are in the vicinity of the nadir point, each sea surface height used in the storm surge measurement was determined by taking the 20 points of each 64-point cross-track sweep that were nearest nadir on each of 20 consecutive scan lines and averaging the elevations of those 400 points whose power levels exceeded the signal threshold. The starting scan line number for successive storm surge measurements was increased by 10 so that there would be a 50% overlap of the data points in adjacent averages. Two examples of the 20 × 20 point areas averaged over are indicated by the black parallelograms near 3 and 13 km in the bottom image of Fig. 5. The averaging areas are small enough so that wave structure will cause the instantaneous water level within the area to deviate from the true mean elevation of the sea surface at that location.

An additional editing criterion was that scan lines were not processed if the roll attitude of the aircraft exceeded 6°. This eliminated the most turbulent regions and times when the aircraft was making significant changes in flight direction.

In addition to the mean water level, the SRA documents the storm waves that cause much of the structural damage and beach erosion. In Fig. 5, the wave topography shows a dramatic spatial variation in the wave

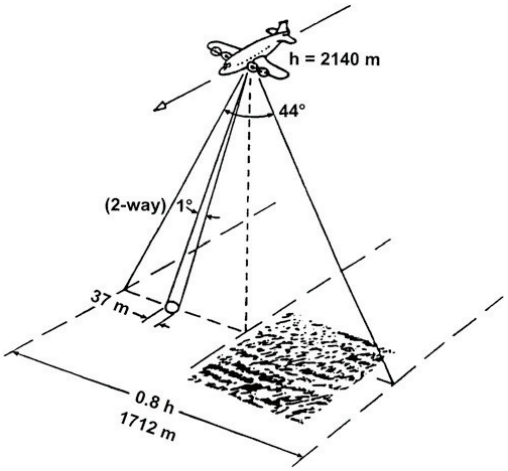

FIG. 4. SRA measurement geometry.

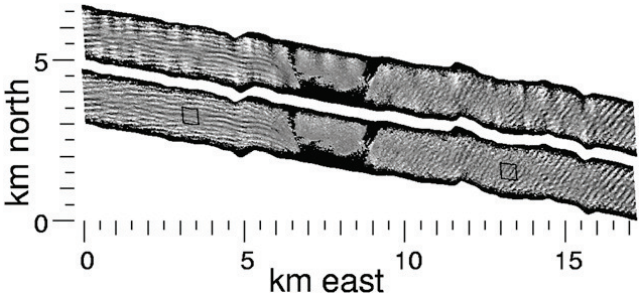

FIG. 5. Grayscale-coded topographic maps produced from 687 SRA raster scan lines as the aircraft crossed Cape Lookout, processed by (top) using the INS roll attitude and (bottom) autoleveling each raster scan line. The landmass occupies the black data dropout region between about 6.5 and 9 km along the abscissa.

field with the waves propagating toward the northwest on the east side of Cape Lookout and toward the north on the west side. Documenting the variation of the directional wave spectrum as a function of distance from shore would also provide additional information on the wave contribution to the surge.

4. Airborne measurement of sea surface elevation

The top panel of Fig. 6 shows the altitude variation indicated by the aircraft data system during a five-hour interval on the 26 August 1998 flight. The height variation spanned 160 m because of changes in atmospheric pressure and updrafts and downdrafts. The precise height variation of the aircraft was determined postflight with a survey-quality differential global positioning system (GPS) trajectory.

The original processing in 1998 produced a trajectory with numerous gaps, one larger than 18 min, because of the large amount of aircraft maneuvering. After the 1998 hurricane season, an actuated antenna mount was developed that would roll the GPS antenna in the opposite direction to the aircraft roll to maintain the antenna boresight vertical. The stabilized antenna greatly improved GPS data quality, but the coverage of a landfalling hurricane was never again as extensive as it was for Hurricane Bonnie. Recently improved processing techniques were able to recover a good-quality aircraft trajectory for the Bonnie landfall flight.

The reference ellipsoid used for the GPS trajectory was the World Geodetic System of 1984 (WGS84), which is slightly different than the T/P ellipsoid. The ellipsoids are defined by two parameters: the semimajor axis and the flattening. The T/P semimajor axis is 6 378 136.3 m and the flattening is 1/298.257. The WGS84 ellipsoid semimajor axis is 6 378 137.0 m and the flattening is 1/298.257 223 563. Because the ellipsoids are rotationally symmetric, their elevations only differ as a function of latitude. WGS84 is higher than T/P by 0.705 m at 36°N and by 0.704 m at 31.5°N.

The initial calibration of the SRA range measurements was done while the aircraft was on the ground using a 45° reflector placed beneath the antenna to divert the beam toward corner reflectors placed at 122-, 183-, and 244-m ranges. Because the SRA antenna looked out the bottom of the aircraft about 4 m below and 4 m aft of the GPS antenna located on top of the aircraft, its precise height in meters was related to the GPS height by $-3.94 - 4.21 \tan(\text{aircraft pitch attitude})$.

Subtracting the vertical distance to the sea surface averaged over 20×20 point areas from the height of the SRA antenna produced the surface elevations with respect to the WGS84 ellipsoid shown in the middle panel of Fig. 6. Because of the GPS trajectory, the 50- and 100-m height excursions in evidence in the top panel did not contaminate the middle panel elevations whose 12-m span was mainly due to the MSS variation shown in Fig. 3. When the 0.7045-m difference of the reference ellipsoids was added and the MSS elevation was subtracted from the elevations of the middle panel, the residual elevation variation (bottom panel) was only about 3 m.

The scatter in the elevation data to the right of point H in the bottom panel of Fig. 6 is significantly greater than the scatter to the right of point F. This does not indicate an increased noise in the SRA range measurements but rather increased deviation of the instantaneous sea surface elevation within the measurement areas from the actual mean sea level resulting from the presence of waves. Figure 3 indicates that the aircraft was traveling north after leaving both points F and H. Walsh et al. (2002, their Figs. 9, 10) indicate that the significant wave height was 4.6 m north of point F and 8.2 m north of point H. There was a trimodal wave system with a 139-m

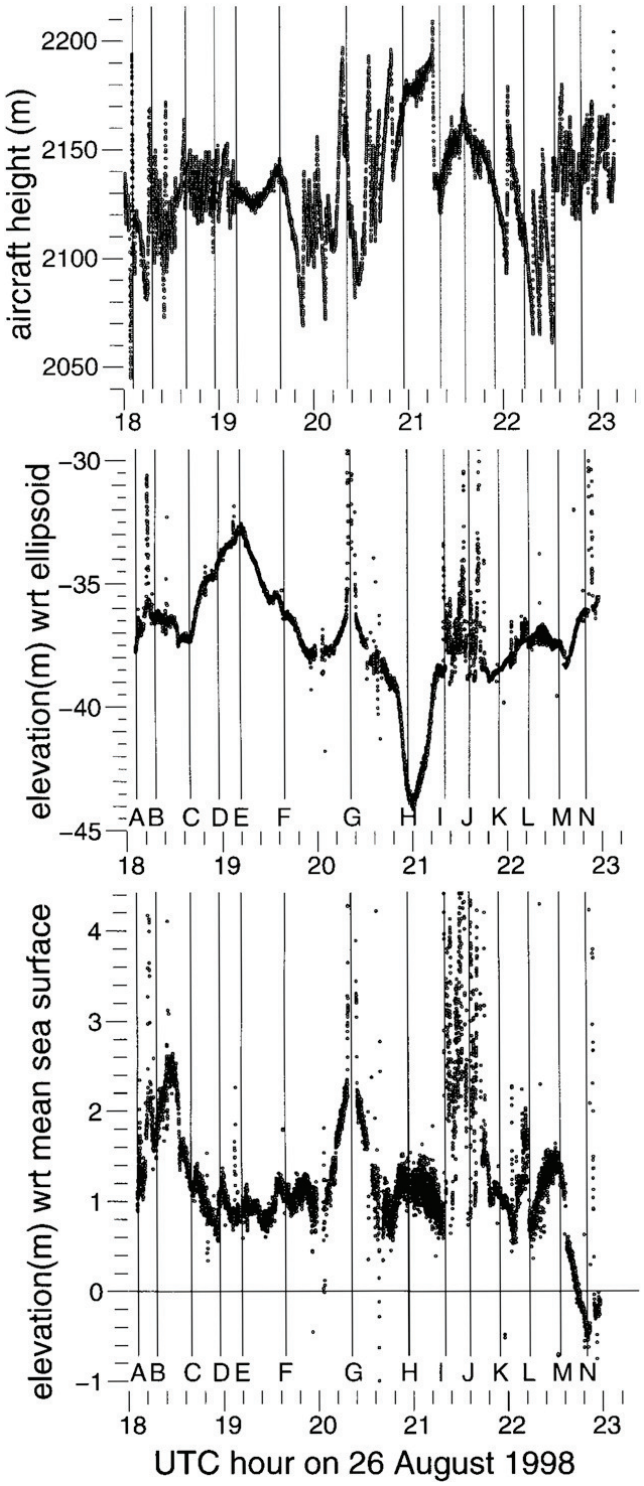

FIG. 6. (top) Aircraft altitude variation along the same track as in Fig. 3, and the SRA determination of sea surface elevation with respect to (middle) the ellipsoid and (bottom) the MSS.

dominant wavelength north of point F and a bimodal wave system with 269-m dominant wavelength north of point H. Higher waves and fewer wavelengths within the averaging area produce greater variability in the instantaneous sea surface elevation. The very high scatter present at point G and from point I to halfway between points J and K was due to land within the SRA swath.

In the bottom panel of Fig. 6, the typical elevation observed by the SRA is about 1 m above the MSS. This is peculiar because Fig. 3 indicates that point F is 200 km offshore and 200 km to the rear of Hurricane Bonnie, and point H is off the continental shelf. It appears that the SRA range calibration performed on the ground was inadequate and the problem was solved by the in-flight calibration described in the next section.

5. In-flight calibration of SRA storm surge measurements

During the Hurricane Bonnie landfall flight, it was considered useful to fly along the shoreline with land occupying half the SRA swath, believing absolute vertical registration could be accomplished by comparing the SRA terrain to lidar surveys conducted by the NASA/Goddard Space Flight Center and the United States Geological Survey. Figure 3 contains such segments between points I and J, halfway between points K and L, near point B, and after point N.

It turned out that the size of the SRA footprint and the high density of man-made structures along the coast made it difficult to compare SRA data with the high-density, small footprint lidar surveys. The torsion in the airframe became a major issue because the SRA swath straddled the shoreline as the aircraft flew from Cape Hatteras, North Carolina, up the coast past the Duck, North Carolina, tide gauge (points I–J in Fig. 3). Having terrain in half the swath made it impossible to determine the true boresight attitude of the antenna. The lost data at Duck made it apparent that for future coastline measurements the aircraft should fly just offshore so the swath contained only water and rely on a high-quality GPS trajectory to determine the aircraft height.

It was fortunate that the SRA did pass by four tide gauges without land contaminating its measurements. Figure 7 shows the water elevations relative to the MSS measured by the SRA as a function of along-track distance relative to the point of closest approach to four tide gauges. Positive distances are to the north of the point of closest approach and negative distances are to the south. The horizontal line in each graph indicates the value assigned to the SRA elevation at the tide gauge location. The vertical scales are identical on the four graphs to facilitate comparison of elevation fluctuations. The fluctuations are similar in the vicinity of the Charleston, South Carolina; Oregon Inlet; and Springmaid Pier tide gauges but significantly larger at Cape Hatteras, where the waves were larger. The significant wave height 15 km south of

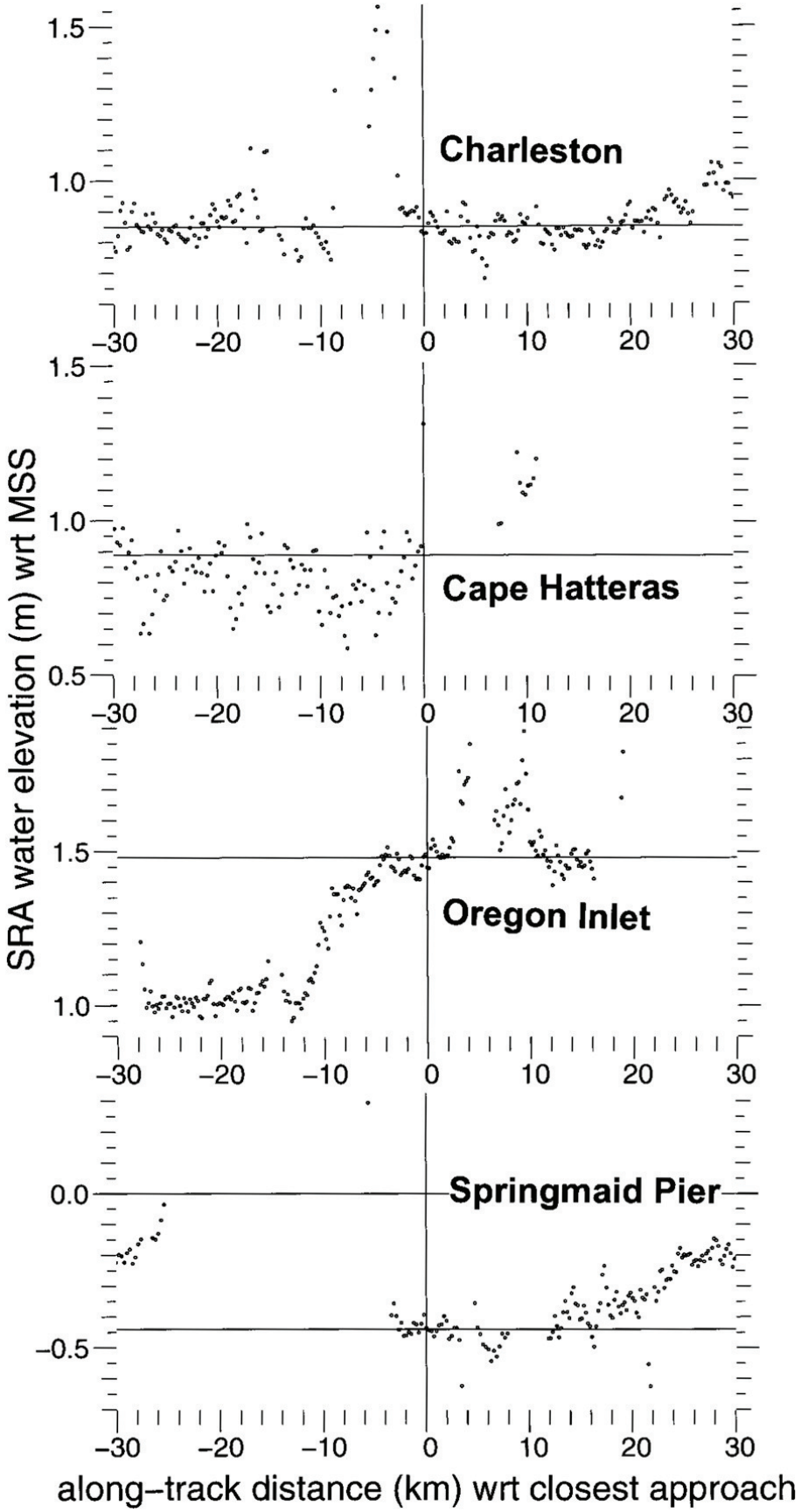

FIG. 7. Water elevations relative to MSS measured by the SRA as a function of along-track distance relative to the point of closest approach to four tide gauges.

TABLE 1. Water elevation with respect to the MSS measured by the tide gauges and the SRA at four locations and the bias that would need to be added to the SRA elevations to bring them into agreement.

Tide gauge	Gauge water elev (m)	SRA water elev (m)	SRA bias (m)
Charleston	−0.17	0.85	−1.02
Cape Hatteras	−0.12	0.89	−1.01
Oregon Inlet	−0.19	1.48	−1.67
Springmaid Pier	−1.47	−0.44	−1.03

Cape Hatteras was still 5 m (Walsh et al. 2002, their Fig. 10I). Only points within 2 km of shore were used in determining the SRA water elevation at Cape Hatteras.

Table 1 lists the tide gauge water elevations relative to MSS, the SRA elevations, and their difference. The difference between the tide gauge and the SRA elevation is within 0.01 m of −1.02 m at Charleston, Cape Hatteras, and Springmaid Pier. The North Carolina State University (NCSU) storm surge model, which will be discussed later, indicated a large gradient between the location of the Oregon Inlet tide gauge and the point of closest approach of the SRA with the water level rising 0.6 m. That would suggest a bias of −1.07 m at Oregon Inlet.

We concluded that the SRA ground calibration was inadequate and that the tide gauge comparisons provided the ultimate calibration of the system, performed at the same altitude, under the same conditions, and in the same manner as the measurements themselves. We have applied a constant −1.03-m bias to all the SRA water elevation measurements made during the landfall flight.

A constant 1-m bias relative to the ground calibration is of little significance because it could be attributed to the sum of multiple sources, such as an error in positioning the corner reflectors and the variation of the speed of light. The SRA processing uses the nominal speed of light at sea level (299 702 547 m s^{-1}). At the 2140-m height of the SRA, that value results in the measured range being shorter (surface elevation higher) by 0.64 m relative to using the speed of light in a vacuum (299 792 458 m s^{-1}).

6. Tidal variation

The 5-h interval shown in Fig. 6 is a significant fraction of a tidal cycle and the predicted value of the water level relative to MSS in the absence of the hurricane must be subtracted from the SRA elevation measurements to arrive at the storm surge. The Beaufort, North Carolina, tide gauge was not used directly because its location at the Duke Marine Laboratory was sheltered from the Atlantic. Its tidal cycle showed a significant lag when compared with the Cape Hatteras gauge and Hess et al. (2005) indicated that its amplitude was significantly lower than in the adjoining Atlantic.

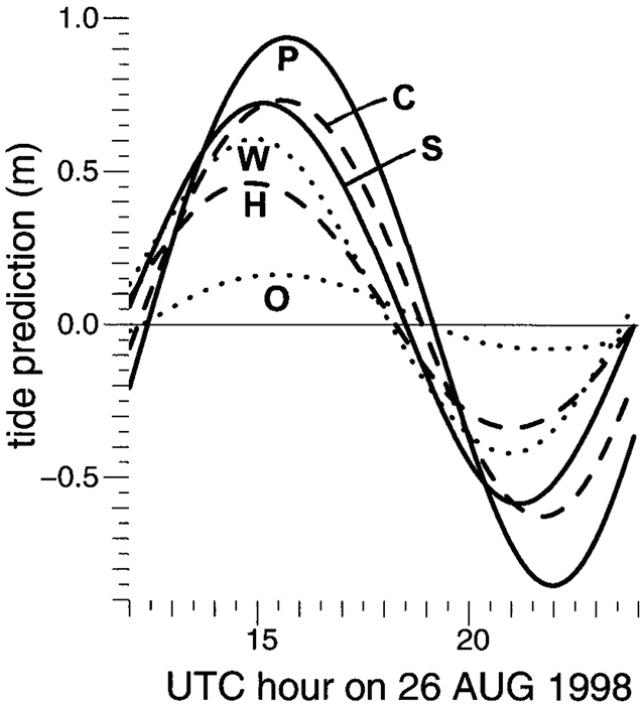

FIG. 8. Tide predictions for Fort Pulaski (P), Charleston (C), Springmaid Pier (S), Wrightsville Beach (W), Cape Hatteras (H), and Oregon Inlet (O).

The tide prediction at Beaufort for 5–7 September 2005 was very similar to the Beaufort prediction for 25–27 August 1998. When the Beaufort prediction for 5–7 September 2005 was multiplied by 1.32 and shifted earlier by 30 min, it almost perfectly matched (1.4-cm rms difference) the prediction for the tide gauge at Wrightsville Beach. That algorithm was used to convert the Beaufort prediction for the Bonnie landfall into a tide prediction for Wrightsville Beach.

Figure 8 shows the tide predictions used to produce storm surge from the SRA surface elevation measurements. As an expedient for data in the Atlantic Ocean, the tidal elevation for each SRA data point was linearly interpolated using longitude and the predictions for Fort Pulaski, Georgia; Charleston; Springmaid Pier; Wrightsville Beach; and Cape Hatteras. The Cape Hatteras longitude was shifted slightly to the east to encompass the aircraft track.

As would be expected, the Oregon Inlet tide prediction is much reduced in amplitude and significantly lags the Cape Hatteras prediction. It was used for the SRA observations in Pamlico Sound and was nearly constant at a value of −0.08 m during the aircraft transit.

7. Storm surge models

Were the spatial and temporal domains of the SRA measurements sufficient to document the storm surge associated with Hurricane Bonnie? Two storm surge models, one operational model used nationally and one research model from the state where the landfall occurred, were used to put the SRA measurements in perspective. Sea, Lake and Overland Surges from Hurricanes (SLOSH), the NOAA operational storm surge model (Glahn et al. 2009; available online at http://www.nhc.noaa.gov/HAW2/english/surge/slosh.shtml), is used by NOAA to forecast storm surge heights resulting from historical, hypothetical, or predicted hurricanes. SLOSH uses fixed internal parameters based on historical storms. NOAA does not tune the parameters for any particular geographic area, nor for a particular storm. The NHC and local National Weather Service (NWS) offices use this information when issuing hurricane advisories.

Wind speed is not an input parameter of the SLOSH model, which calculates the wind field from the central barometric pressure and radius of maximum wind. Jelesnianski et al. (1992) developed the parametric wind model used by SLOSH and they describe it and the surge model in detail. The surface wind field is first computed via their solution of a differential equation for a symmetric hurricane. Both the wind speed and direction result from this formulation. To account for asymmetry, one-half of the forward speed is added vectorially to the wind field. The one-half factor was empirically established by examining past hurricanes. Using the full forward speed caused winds for New England hurricanes to be erroneous on both the left and right sides of the hurricane.

The NCSU research model (Peng et al. 2004; Xie et al. 2004, 2006; Peng et al. 2006) is a mass-conserving interactive inundation and drying scheme incorporated into a three-dimensional coastal ocean and estuarine circulation model. It uses asymmetric wind forcing by incorporating an asymmetry term into the Holland hurricane wind field model (Holland 1980), enhanced by using any available near-real-time data to optimize the model parameters.

SLOSH and NCSU model results were provided without knowledge of the other model output or the SRA observations. Model output was requested for the period 1700–2300 UTC 26 August 1998 for the region between 33° and 36°N and 79.4° and 75.4°W. The NCSU storm surge elevations were supplied at 1-h intervals in that domain on a rectangular grid with a 2-arc min resolution.

SLOSH uses telescoping grids centered in different geographical areas to cover large areas with detailed land topography. The complex grids indicate the water level in approximately square areas whose orientation and size vary with the distance and direction from the origin. SLOSH outputs were supplied for both the Wilmington/Myrtle Beach Basin (South Carolina) and the Pamlico Sound Basin. At the shoreline in the middle of Onslow Bay, North Carolina, the areas were approximately 1.5 km on each side and at Myrtle Beach they were 1 km on each side. In the middle of Pamlico Sound, the areas were about 2.2 km on each side. This is somewhat smaller than the 3.7 km $\times$ 3 km constant gridpoint spacing of the surge data from the NCSU model.

The SLOSH outputs supplied were from standard poststorm runs, similar to what is done in NWS operations, but with the NHC poststorm best-track position, size, and intensity. They covered the period from 1100 UTC on 25 August through 1700 on 28 August with a 20-min temporal interval in the Wilmington/Myrtle Beach Basin and a 15-min interval in the Pamlico Sound Basin. The SLOSH water elevations supplied were the sum of the storm surge and a tidal component, which was constant both temporally and spatially at 0.61 m in the Atlantic Ocean and 0.15 m in Pamlico Sound. Those tidal values were subtracted from the SLOSH water elevations to arrive at the surge values.

SLOSH indicated that the surge peaked at 1.5 m on the east side of Cape Fear at 1330 UTC and then slowly diminished as it shifted up along the North Carolina coast in Onslow Bay, reaching Browns Inlet (34.59°N, 77.23°W) at 2300 UTC with a value of 1.2 m. The SRA measured the surge in that region 3 times at about 2-h intervals.

8. SRA storm surge measurements

The top panel of Fig. 9 superimposes the SLOSH and NCSU storm surge contours and the aircraft track, which began east of Cape Lookout at 1806 UTC and approached Cape Island, South Carolina, at 1857 UTC (points A, B, C, and D in Fig. 3). Two things stand out. First, the orientation of the surge elevation contours in Onslow Bay for SLOSH is about 56°, roughly 18° counterclockwise from the NCSU contours. Second, the NCSU model indicates a depressed water level west of Cape Fear, where the SLOSH surge does not even diminish to 0.3 m.

The bottom panel of Fig. 9 indicates the NCSU surge values along the flight track, interpolated in both time and space from the 1-h datasets provided. The SLOSH graphical display option by which individual locations can be interrogated for elevation was used to determine

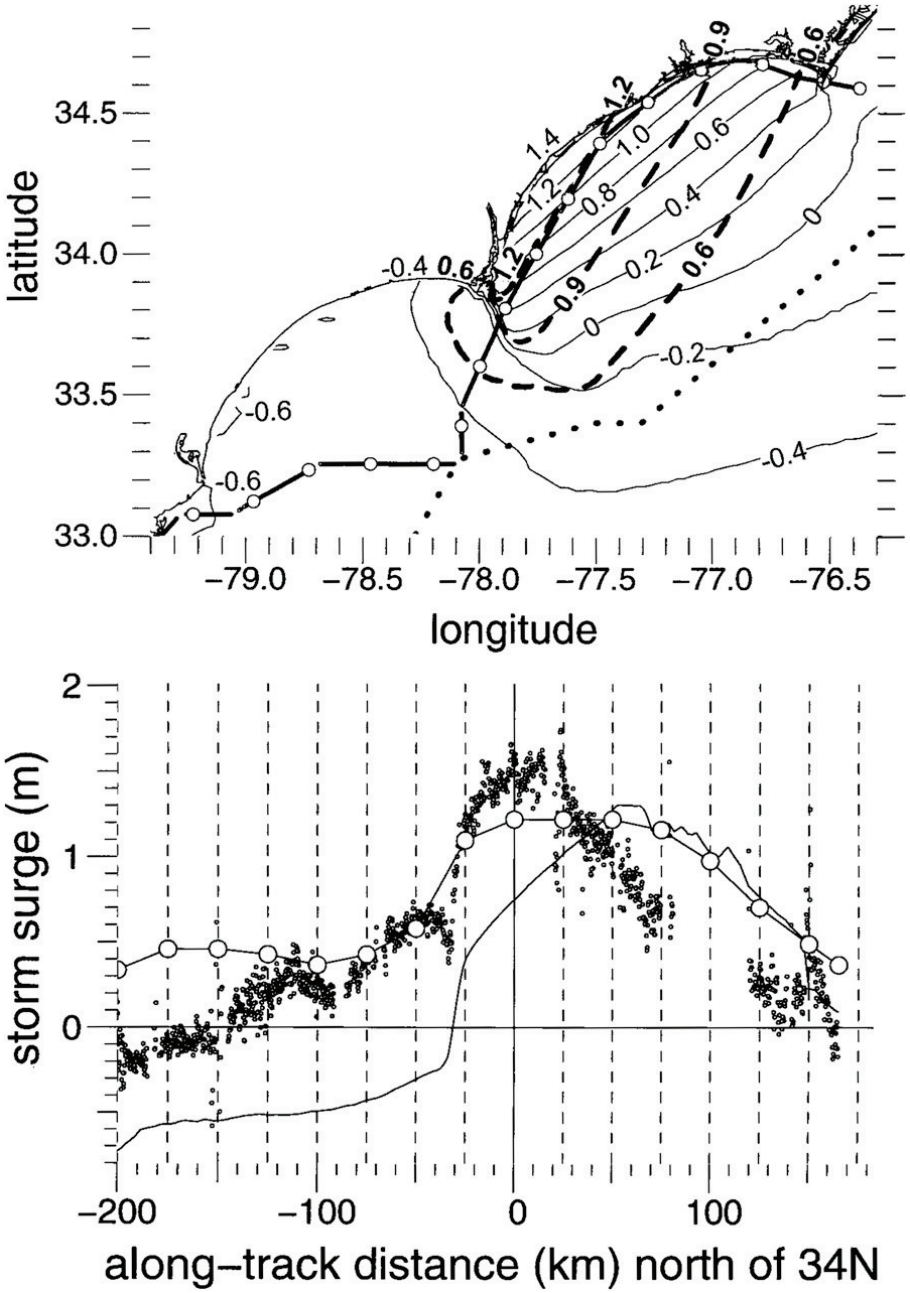

FIG. 9. (top) Circles identify positions along the aircraft track spaced at 25-km intervals (except for the first point) relative to passing 34°N. The thin lines indicate the NCSU storm surge contours at 1828 UTC, when the aircraft passed through 34°N. The thick dashed lines indicate the SLOSH storm surge contours at 1820 UTC. Dots indicate a piecewise linear approximation of the western edge of the Gulf Stream. (bottom) Dots indicate SRA storm surge values along the flight track. The curve without the circles indicates the NCSU surge values along the flight track. SLOSH surge values are indicated by the circles connected by straight line segments.

the surge at the positions indicated by the circles in the top panel. Those values for SLOSH are indicated by the circles in the bottom panel and connected by line segments.

The dots in the bottom panel of Fig. 9 indicate the SRA storm surge values along the flight track, each being the average of up to 400 individual elevations (20×20 grid near nadir whose power values exceed a threshold; parallelograms in Fig. 5, bottom image). With a few exceptions, the SRA surge values in Fig. 9 cluster tightly about their mean trend. The gap in the SRA data in the

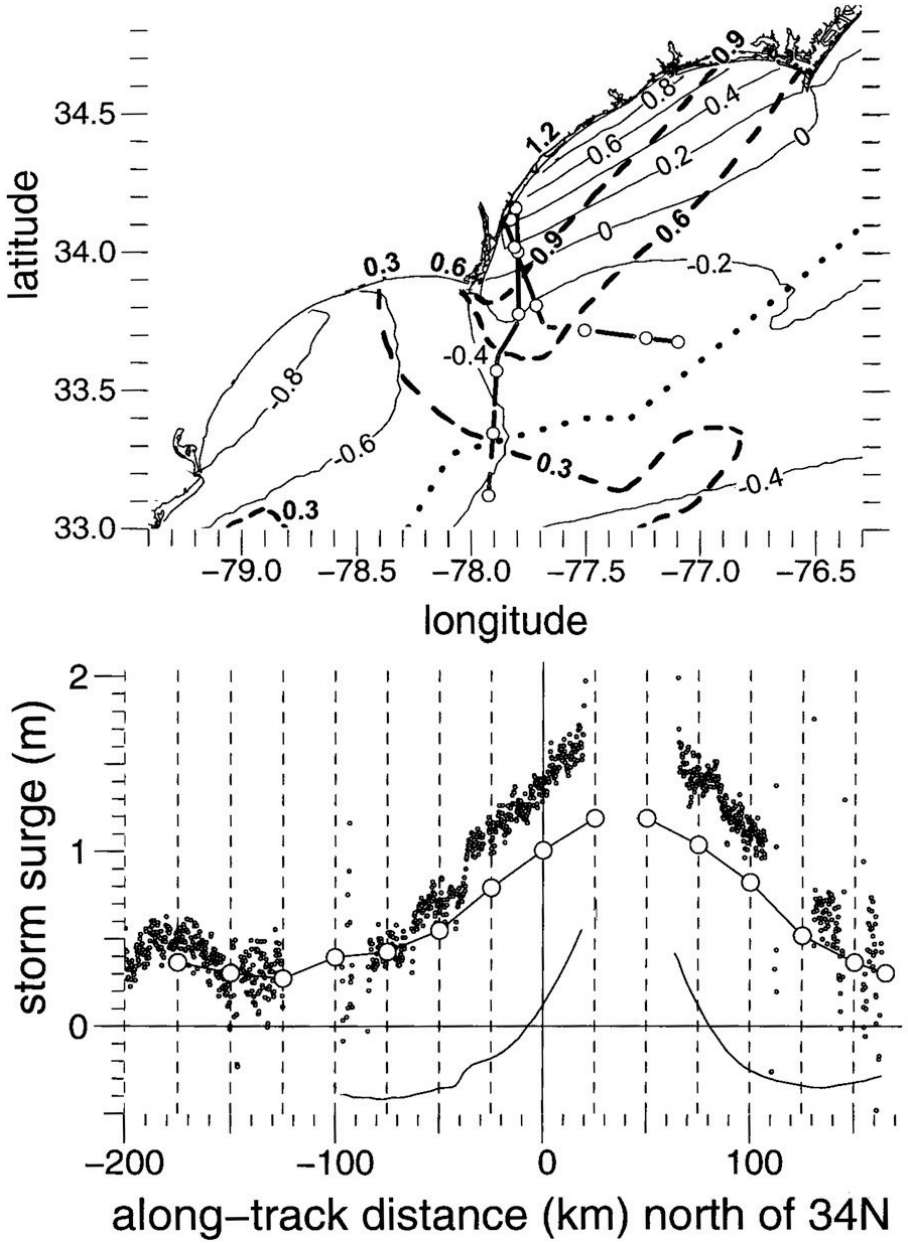

FIG. 10. (top) Circles are spaced at 25-km intervals along the aircraft track (except for the last one) relative to the aircraft first reaching 34°N flying north at 2016 UTC. The thin lines indicate the NCSU storm surge contours at 2016 UTC. The thick dashed lines indicate the SLOSH storm surge contours at 2020 UTC. Dots indicate a piecewise linear approximation of the western edge of the Gulf Stream. (bottom) Dots indicate SRA storm surge values along the flight track. The curve without the circles indicates NCSU surge values along the flight track. SLOSH surge values are indicated by the circles connected by line segments.

region between 80 and 120 km north of 34°N is due to land contamination.

Both models indicate a peak surge along the flight line of about 1.2 m, but NCSU suggests that the maximum would occur farther north than SLOSH. The SRA indicates a maximum surge of 1.5 m at about 34°N. About 65 km of the aircraft track were nearly along the 1.2-m SLOSH contour. The SRA surge increasing along that segment suggests that the contours of constant surge were actually rotated even more counterclockwise than the SLOSH contours.

South of Cape Fear, NCSU indicates that the surge decreases much more rapidly than either SLOSH or the SRA. By the time the aircraft approached Cape Island (−200 km), the SRA storm surge had become negative and was about halfway between SLOSH and NCSU.

Figure 10 shows the situation about 2 h later. The aircraft had left point F (Fig. 3) and flown north until reaching 33.6°N, where it diverted slightly to the east and flew north to intercept the coast near Wrightsville Beach. It then looped around to the west and flew south-southeast back over the water before turning east. The aircraft first reached 34°N, flying north at 2016 UTC.

In the 2 h since the data shown in Fig. 9, the SLOSH elevation contours in Onslow Bay rotated about 10° clockwise to about 46°. The NCSU contours also rotated, maintaining approximately the same angle between the two models. NCSU indicates the water depression west of Cape Fear deepened but the SLOSH surge was still positive.

The along-track distances in the bottom panel of Fig. 10 are relative to the initial crossing of 34°N while flying north. The second time the aircraft passed through 34°N, flying south-southeast, occurred at the 75-km point. The NCSU domain requested only extended to 33°N (−114 km in the bottom panel plot) and there were no SRA data in the −100 to −125-km interval because of rain attenuation. SLOSH was in quite good agreement with the SRA surge values in the interval of −200 to −75 km (<33.35°N), but it was about 0.5 m low for the surge at the coastline. NCSU indicated that the sea surface was depressed at Cape Fear and to the south.

During the third interrogation of the area off Wrightsville Beach shown in Fig. 11, the aircraft left Cape Lookout and flew down around Cape Fear and into Myrtle Beach (points L, M, N in Fig. 3, respectively). It passed through 34°N at 2232 UTC. The SLOSH elevation contours in Onslow Bay had rotated another 10° clockwise to about 36°. The NCSU contours had also rotated, maintaining approximately the same angle between the two models. SLOSH indicated that the water surface was depressed starting about halfway between Cape Fear and Myrtle Beach. The SRA surge was lower than both models just west of Cape Lookout (as it was in Fig. 9), was comparable to SLOSH near Wrightsville Beach, then plummeted near Cape Fear and was closer to NCSU at Myrtle Beach and Springmaid Pier.

The rise in the SRA surge level between 125 and 50 km suggests that the contours of constant surge level were still rotated counterclockwise relative to the SLOSH contours, similar to the situation in the bottom of Fig. 9. The SLOSH Onslow Bay surge at 34°N decayed steadily (1.2, 1.0, and 0.76 m) over the 4-h interval of Figs. 9–11 while the SRA surge was nearly constant initially and then decreased rapidly (1.5, 1.4, and 0.7 m).

The top of Fig. 12 shows the SRA track in Pamlico Sound, which passed through 35.4°N at 2155 UTC. The NCSU contours of constant surge are rotated clockwise relative to SLOSH, but the angle between them is about 3 times greater than it was in Onslow Bay.

Although both models indicate a maximum surge of about 1.7 m in Pamlico Sound, the almost north–south orientation of the SLOSH contours predict an increasing surge level as the aircraft track progresses from north to south (25 to −40 km in Fig. 12, bottom), which is not supported by the SRA. NCSU indicates a decreasing surge level along that segment that agrees with the SRA trend, but the SRA measurements are well below the NCSU predictions.

9. Discussion

Figures 9–12 indicate that an airborne wide-swath radar altimeter can produce very low noise measurements of the storm surge associated with a landfalling hurricane that could be used to evaluate and improve model performance. Figure 13 suggests that the first-order differences between the SRA measurements and the two surge models in Onslow Bay may have been caused by the different tracks the models used for Hurricane Bonnie. The SLOSH track (dashes) was determined by a spline fit through the NHC 6-h-interval best-track storm positions (X). NCSU used the eye locations (dots) at two-hour intervals issued in the NHC advisories during landfall.

After 1200 UTC, the NCSU track speeds up and then diverts about 25 km to the west as it approaches Cape Fear compared to the best track. The NHC 2-h advisories placed Bonnie at 33.7°N at 1900 UTC, whereas the SRA aircraft suggested that it did not reach that latitude until 2000 UTC and the best track indicated 2100 UTC, a 2-h spread. The NHC 2-h advisories placed Bonnie at 34°N at 2100 UTC, whereas the SRA aircraft suggested that it did not reach that latitude until about 2300 UTC and the best track indicated 2400 UTC, a 3-h spread.

In addition to the aircraft eye fixes indicating a forward speed for Bonnie between that used by SLOSH and NCSU, two of the aircraft eye locations were between the tracks used by the models, which might also help explain why the SRA surge was sometimes between the models.

Dashed radials extend from the 2100 UTC eye locations on the two tracks to Springmaid Pier and to the middle on Onslow Bay. Arrows drawn from the Springmaid Pier and Onslow Bay locations at right angles to the dashed radials provide a simple indication of differences in the local downwind direction caused by the track differences.

In the middle of Onslow Bay, the downwind direction for NCSU would have been rotated 30° clockwise from

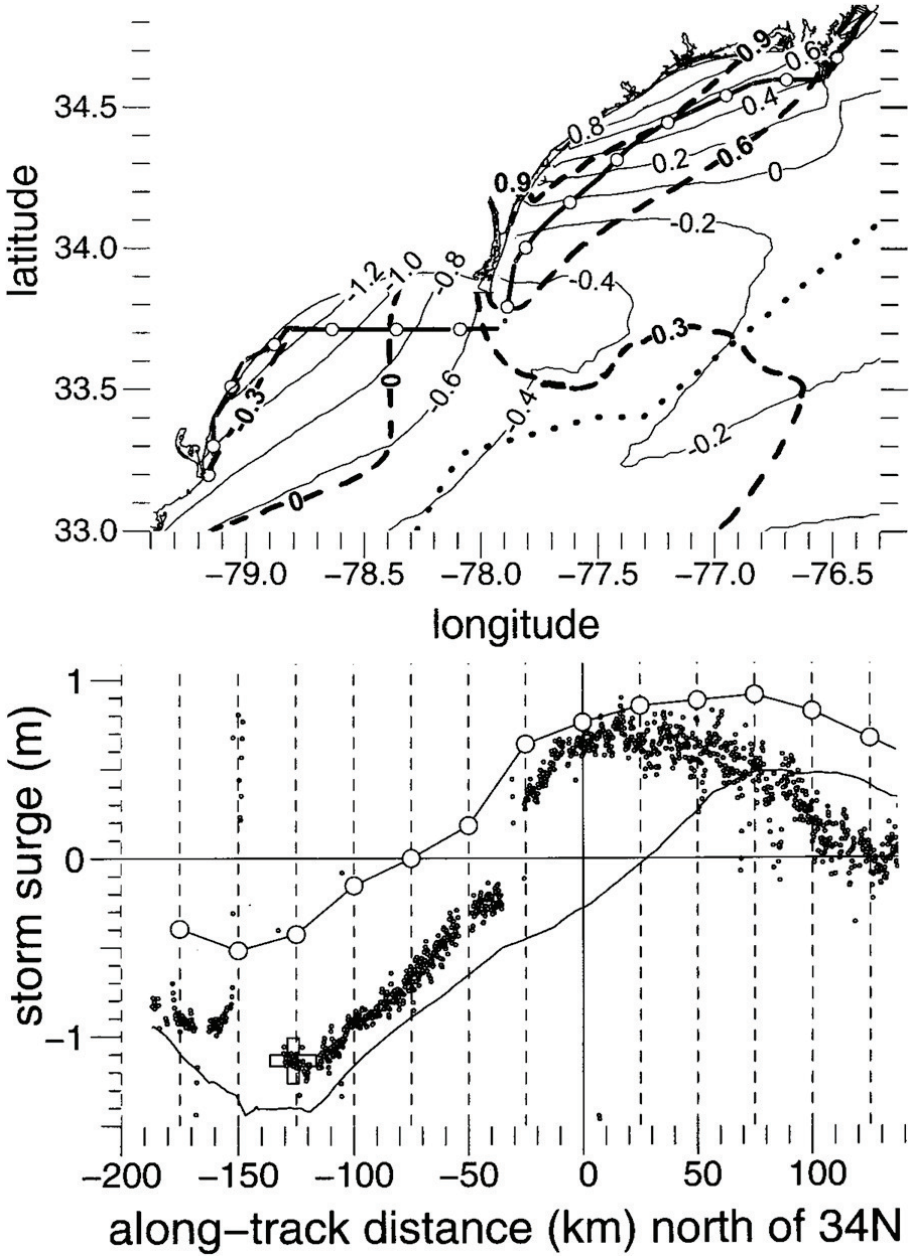

FIG. 11. (top) Circles are spaced at 25-km intervals along the aircraft track relative to the aircraft reaching 34°N flying south at 2232 UTC. The thin lines indicate the NCSU storm surge contours at 2232 UTC, and the thick dashed lines indicate the SLOSH storm surge contours at 2240 UTC. Dots indicate a piecewise linear approximation of the western edge of the Gulf Stream. (bottom) Dots indicate SRA storm surge values along the flight track. The curve without the circles indicates NCSU surge values along the flight track. SLOSH surge values are indicated by the circles connected by line segments.

SLOSH, which was greater than the 18° clockwise rotation in the surge elevation contours shown in the top panels of Figs. 9–11. At Springmaid Pier, the NCSU downwind direction would have been 21° closer to being perpendicular to the shoreline and presumably more effective in producing a depressed water surface. Halfway between Springmaid Pier and Cape Fear, the NCSU downwind direction would have been directly offshore, whereas SLOSH would have been 33° from being perpendicular to the shoreline.

In Pamlico Sound (Fig. 12), the difference in the orientations of the model contours was more dramatic than in Onslow Bay and more difficult to explain by the difference in tracks because its span ranged from 200 to

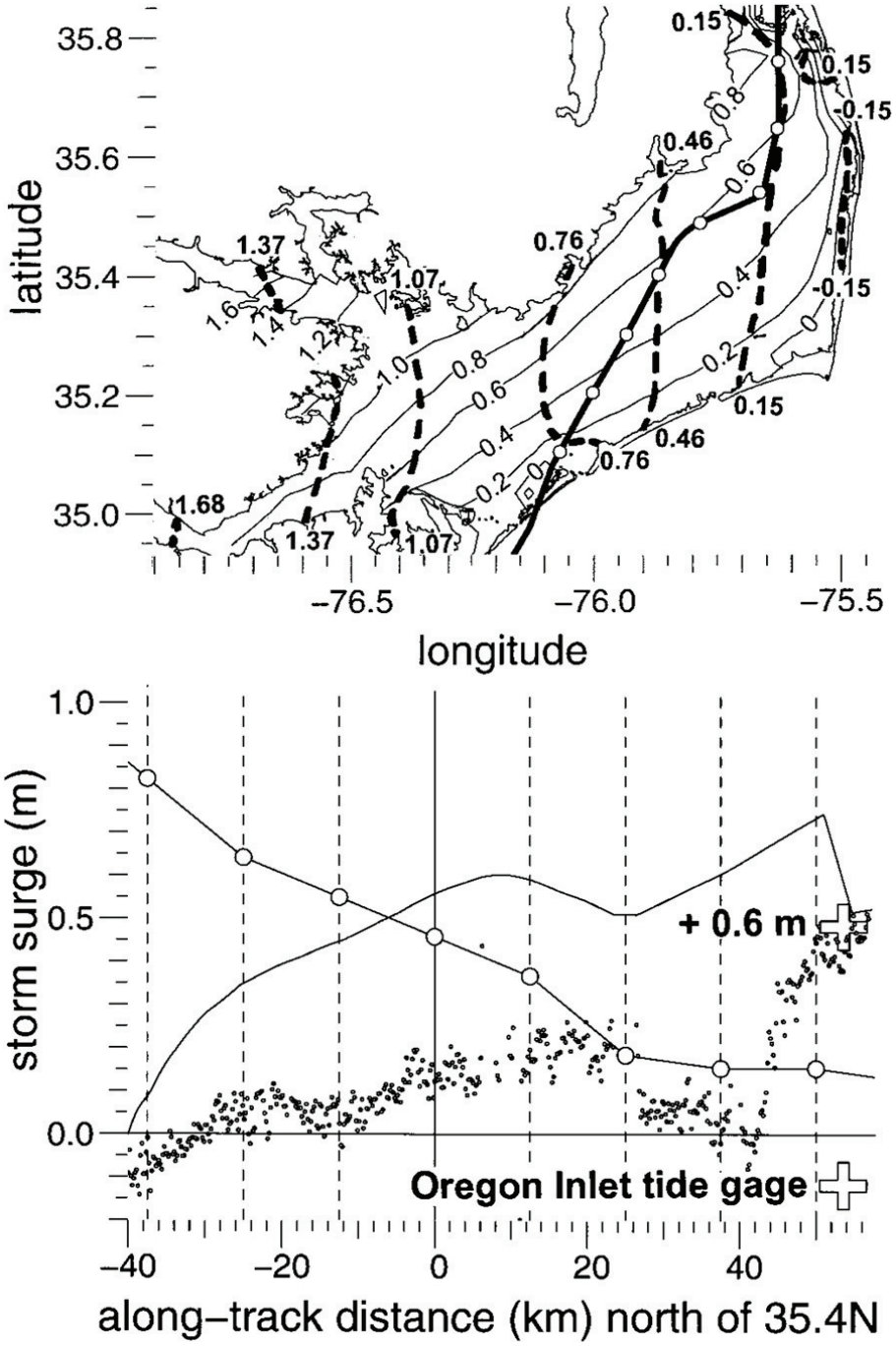

FIG. 12. (top) Circles are spaced at 12.5-km intervals along the aircraft track relative to the aircraft reaching 35.4°N at 2155 UTC flying south in Pamlico Sound. Thin lines indicate the NCSU storm surge contours interpolated to that time, and thick dashed lines indicate the SLOSH storm surge contours at 2200 UTC. (bottom) Dots indicate SRA storm surge values along the flight track. The curve without the circles indicates NCSU surge values along the flight track. SLOSH surge values are indicated by the circles connected by line segments.

300 km from the eye. And the SRA indicated a surge that was generally lower than in either of the models.

It may be that the shallow water and limited access to the ocean make Pamlico Sound a more challenging area to model, but it was beyond the scope of this paper to delve into the details of the model wind fields, physics, or implementations to try to reconcile differences. The low noise level on the SRA measurements suggests that a carefully planned experiment could provide a comprehensive dataset that could serve that purpose. Three

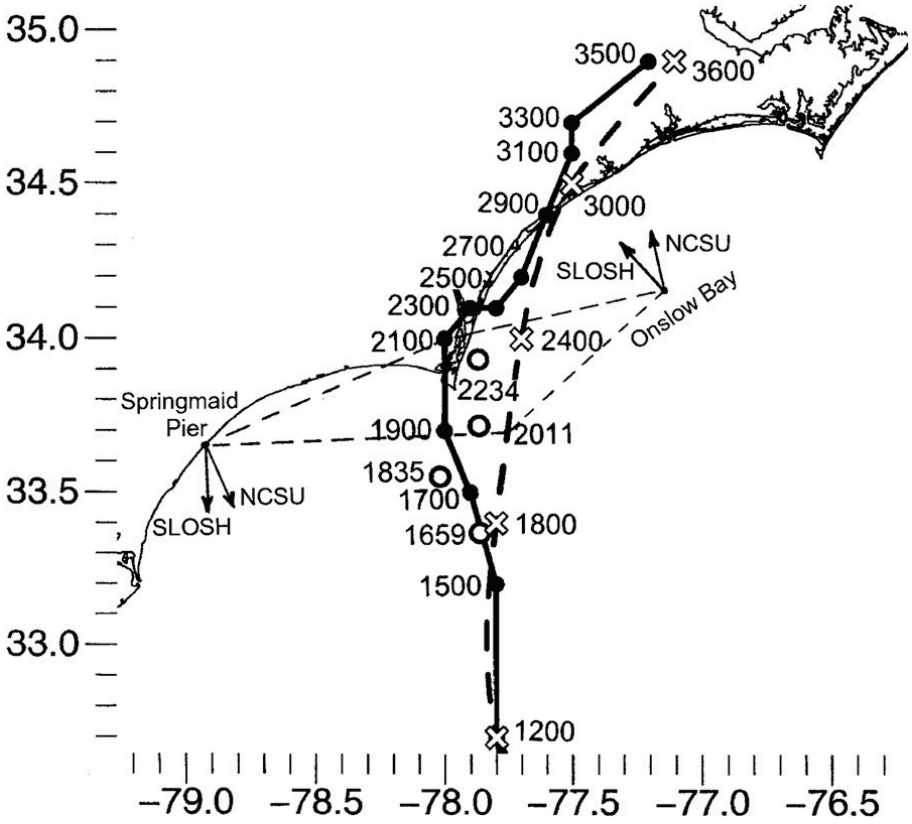

FIG. 13. NHC best-track storm positions (X) and the eye locations (dots) from NHC advisories issued during landfall with time incrementing from 0000 UTC 26 Aug 1998. The four circles indicate eye locations recorded in the N43RF flight director's log (B. Damiano NOAA/AOC, 2007, personal communication) from eye penetrations at 1659, 1835, 2011, and 2234 UTC. Arrows indicate approximate downwind directions in Onslow Bay and at Springmaid Pier for the eye locations used by SLOSH and NCSU at 2100 UTC.

passes through Pamlico Sound in quick succession—1) southwest from 35.55°N, 75.5°W and up the Meuse River to 34.95°N, 76.8°W; 2) southeast from 35.45°N, 76.9°W and down the Pamlico River to 35.15°N, 75.85°W; and then 3) north to 35.6°N, 75.85°W—would document the water level gradients and provide two crossing points to confirm absolute accuracy.

The NASA SRA was decommissioned after the 2005 hurricane season. The NOAA Small Business Innovation Research (SBIR) program subsequently contracted with ProSensing, Inc. (available online at http://www.prosensing.com) to build the Wide-Swath Radar Altimeter (WSRA) to replace it. The WSRA, with improved data quality and less susceptibility to rain attenuation, will be operational for the 2009 hurricane season and beyond. The actuated GPS antenna mount developed by NASA after the 1998 season has been transferred to NOAA for use with the WSRA so that the quality of the GPS data will be better than for Hurricane Bonnie.

More tide gauges are in operation now and a new MSS model should soon be available that will have improved resolution and accuracy over the one employed in the present analysis. There are several tide gauges in Tampa Bay, Florida, which could provide in-flight calibration for the aircraft returning to the NOAA Aircraft Operations Center at MacDill Air Force Base in Tampa, Florida, after a storm surge mission, in addition to any tide gauges that might be in the vicinity of the landfall. With survey-quality GPS trajectories for the aircraft, the new NOAA WSRA could produce targeted measurements of storm surge that would provide an absolute standard for assessing and improving the performance of numerical storm surge models.

Acknowledgments. These measurements and this analysis were supported by the NASA Physical Oceanography Program. The analysis was also supported by the Joint Hurricane Testbed of the NOAA/U.S. Weather Research Program (USWRP) at the Tropical Prediction Center/National Hurricane Center. Donald E. Hines maintained the NASA SRA, and the NOAA Aircraft Operations Center is thanked for their expertise in

helping install the system and executing the complex flight patterns. E. J. Walsh thanks Hendrik Tolman of NCEP for useful discussion.

REFERENCES

Black, P. G., and Coauthors, 2007: Air–sea exchange in hurricanes: Synthesis of observations from the Coupled Boundary Layer Air–Sea Transfer experiment. *Bull. Amer. Meteor. Soc.,* **88,** 357–374.

Fan, Y., I. Ginis, T. Hara, C. W. Wright, and E. J. Walsh, 2009: Numerical simulations and observations of surface wave fields under an extreme tropical cyclone. *J. Phys. Oceanogr.,* **39,** 2097–2116.

FEMA, 2006: Final coastal and riverine high water mark collection for Hurricane Katrina in Mississippi. Federal Emergency Management Agency Final Rep. FEMA-1604-DR-MS, 76 pp. [Available online at http://www.fema.gov/pdf/hazard/flood/recoverydata/katrina/katrina_ms_hwm_public.pdf.]

Fritz, H. M., and Coauthors, 2007: Hurricane Katrina storm surge distribution and field observations on the Mississippi barrier islands. *Estuarine Coastal Shelf Sci.,* **74,** 12–20.

Glahn, R., A. A. Taylor, N. Kurkowski, and W. A. Shaffer, 2009: The role of the SLOSH model in National Weather Service storm surge forecasting. *Natl. Wea. Dig.,* in press.

Hess, K. W., E. Spargo, A. Wong, S. A. White, and S. Gill, 2005: VDatum for central coastal North Carolina: Tidal datums, marine grids, and sea surface topography. NOAA Tech. Rep. NOS CS 21, 56 pp.

Holland, G. J., 1980: An analytic model of the wind and pressure profiles in hurricanes. *Mon. Wea. Rev.,* **108,** 1212–1218.

Jelesnianski, C. P., J. Chen, and W. A. Shaffer, 1992: SLOSH: Sea, Lake, and Overland Surges from Hurricanes. NOAA Tech. Rep. NWS 48, 71 pp.

Moon, I.-J., I. Ginis, T. Hara, H. L. Tolman, C. W. Wright, and E. J. Walsh, 2003: Numerical simulation of sea surface directional wave spectra under hurricane wind forcing. *J. Phys. Oceanogr.,* **33,** 1680–1706.

Peng, M., L. Xie, and J. Pietrafesa, 2004: A numerical study of storm surge and inundation in the Croatan-Albemarle-Pamlico Estuary System. *Estuarine Coastal Shelf Sci.,* **59,** 121–137.

——, ——, and ——, 2006: A numerical study on hurricane-induced storm surge and inundation in Charleston Harbor, South Carolina. *J. Geophys. Res.,* **111,** C08017, doi:10.1029/2004JC002755.

Powell, M. D., S. H. Houston, L. R. Amat, and N. Morisseau-Leroy, 1998: The HRD real-time hurricane wind analysis system. *J. Wind Eng. Ind. Aerodyn.,* **77–78,** 53–64.

——, P. J. Vickery, and T. A. Reinhold, 2003: Reduced drag coefficient for high wind speeds in tropical cyclones. *Nature,* **422,** 279–283.

Schroeder, J. L., and D. A. Smith, 2003: Hurricane Bonnie wind flow characteristics. *J. Wind Eng. Ind. Aerodyn.,* **91,** 767–789.

Tapley, B. D., and Coauthors, 1994: Precision orbit determination for TOPEX/POSEIDON. *J. Geophys. Res.,* **99,** 24 383–24 404.

Uhlhorn, E. W., and P. G. Black, 2003: Verification of remotely sensed sea surface winds in hurricanes. *J. Atmos. Oceanic Technol.,* **20,** 99–116.

——, ——, J. L. Franklin, M. Goodberlet, J. Carswell, and A. S. Goldstein, 2007: Hurricane surface wind measurements from an operational stepped frequency microwave radiometer. *Mon. Wea. Rev.,* **135,** 3070–3085.

Walsh, E. J., D. W. Hancock, D. E. Hines, R. N. Swift, and J. F. Scott, 1985: Directional wave spectra measured with the surface contour radar. *J. Phys. Oceanogr.,* **15,** 566–592.

——, ——, ——, ——, and ——, 1989: An observation of the directional wave spectrum evolution from shoreline to fully developed. *J. Phys. Oceanogr.,* **19,** 670–690.

——, L. K. Shay, H. C. Graber, A. Guillaume, D. Vandemark, D. E. Hines, R. N. Swift, and J. F. Scott, 1996: Observations of surface wave-current interaction during SWADE. *Global Atmos. Ocean Syst.,* **5,** 99–124.

——, and Coauthors, 2002: Hurricane directional wave spectrum spatial variation at landfall. *J. Phys. Oceanogr.,* **32,** 1667–1684.

Wang, Y. M., 2001: GSFC00 mean sea surface, gravity anomaly, and vertical gravity gradient from satellite altimeter data. *J. Geophys. Res.,* **106,** 31 167–31 174.

Wright, C. W., and Coauthors, 2001: Hurricane directional wave spectrum spatial variation in the open ocean. *J. Phys. Oceanogr.,* **31,** 2472–2488.

Xie, L., L. J. Pietrafesa, and M. Peng, 2004: Incorporation of a mass-conserving inundation scheme into a three dimensional storm surge model. *J. Coastal Res.,* **20,** 1209–1223.

——, S. Bao, L. J. Pietrafesa, K. Foley, and M. Fuentes, 2006: A real-time hurricane surface wind forecasting model: Formulation and verification. *Mon. Wea. Rev.,* **134,** 1355–1370.